

AGRADECIMENTOS

EMBRAPA-CNPDIÁ SÃO CARLOS

TODO O PESSOAL , EM PARTICULAR OS AMIGOS :

SERGIO MASCARENHAS (GRANDE AMIGO E «DEUS EX MACHINA»)

SILVIO CRESTANA («deus ex machina» adjunto)

PAULO CRUVINEL (JUÇA)

PAULO HERRMANN

JOÃO DE MENDONÇA NAIME, chefe geral da EMBRAPA-CNPDIÁ

LADISLAU MARTIN NETO, presidente do SIAGRO 2019

UNIVERSIDADE FEDERAL DO RIO DE JANEIRO

RICARDO T. LOPES E COLLEGAS

UNIVERSIDADE ESTADUAL DO RIO DE JANEIRO

JOAQUIM T. DE ASSIS

UNIVERSIDADE DE LONDRINA

CARLOS R. APPOLONI e colaboradores

USP SÃO PAULO

MARCIA RIZZUTTO

UNIVERSIDAD NACIÓN MAYOR DE SAN MARCOS, LIMA PERU

ANGEL BUSTAMANTE e colaboradores.

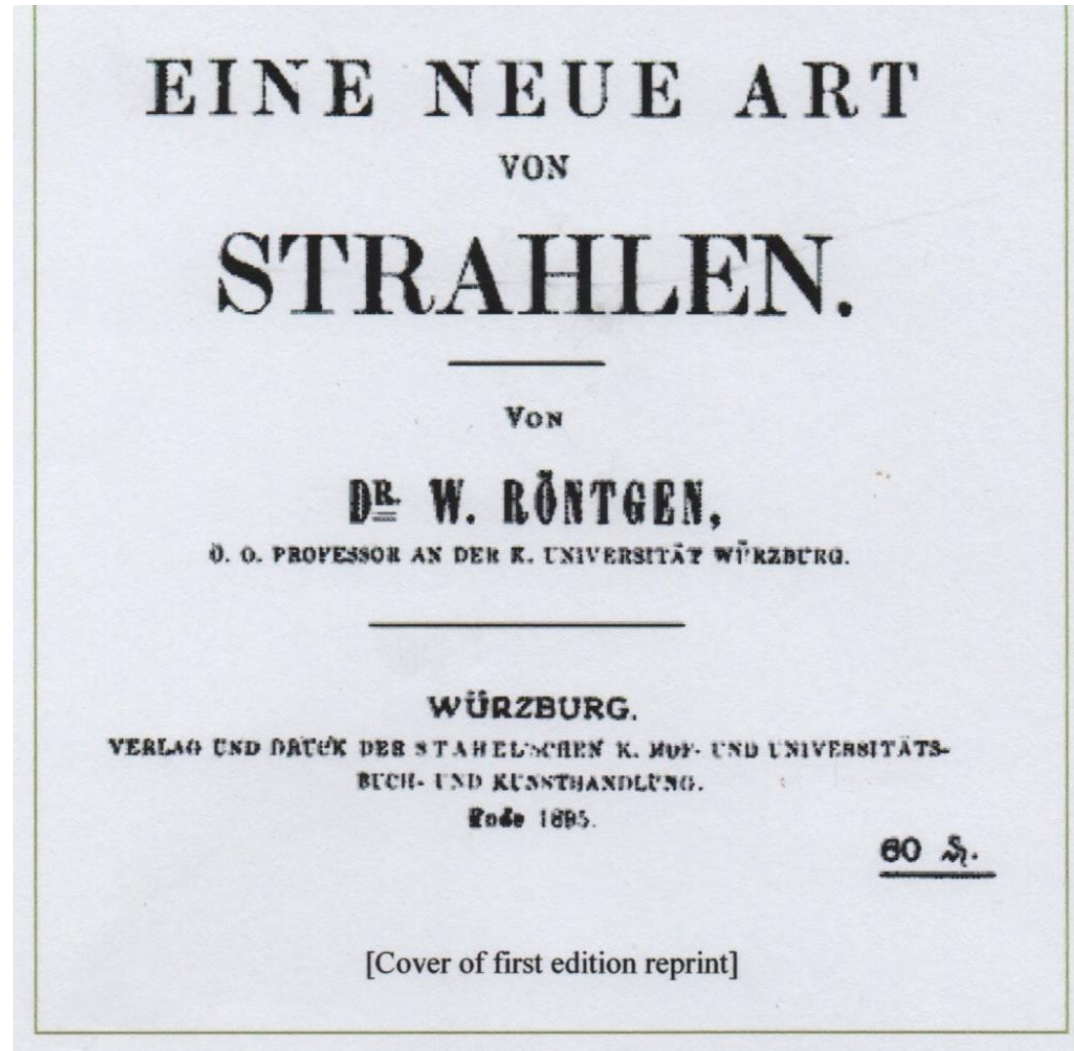


Wilhelm Conrad Röntgen

1845–1923

X – RAYS

WILHELM CONRAD RONTGEN NOBEL PRIZE FOR PHYSICS IN 1901



[Cover of first edition reprint]

FIRST PUBLICATION OF W.C.Röntgen about the discovery of X-rays
(december 1895 in Würzburg) .

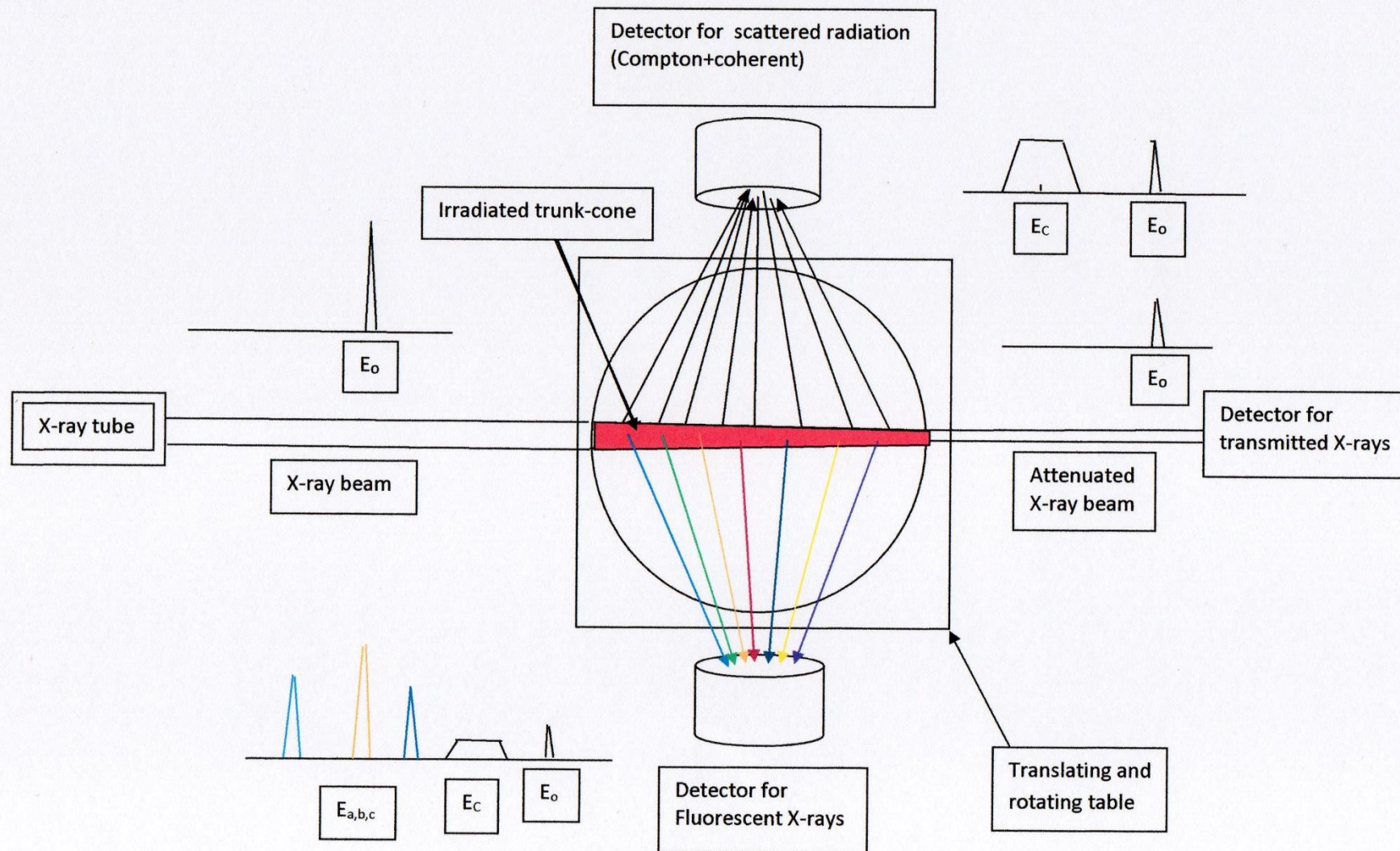
NOBEL PRIZES RELATED TO X-RAYS

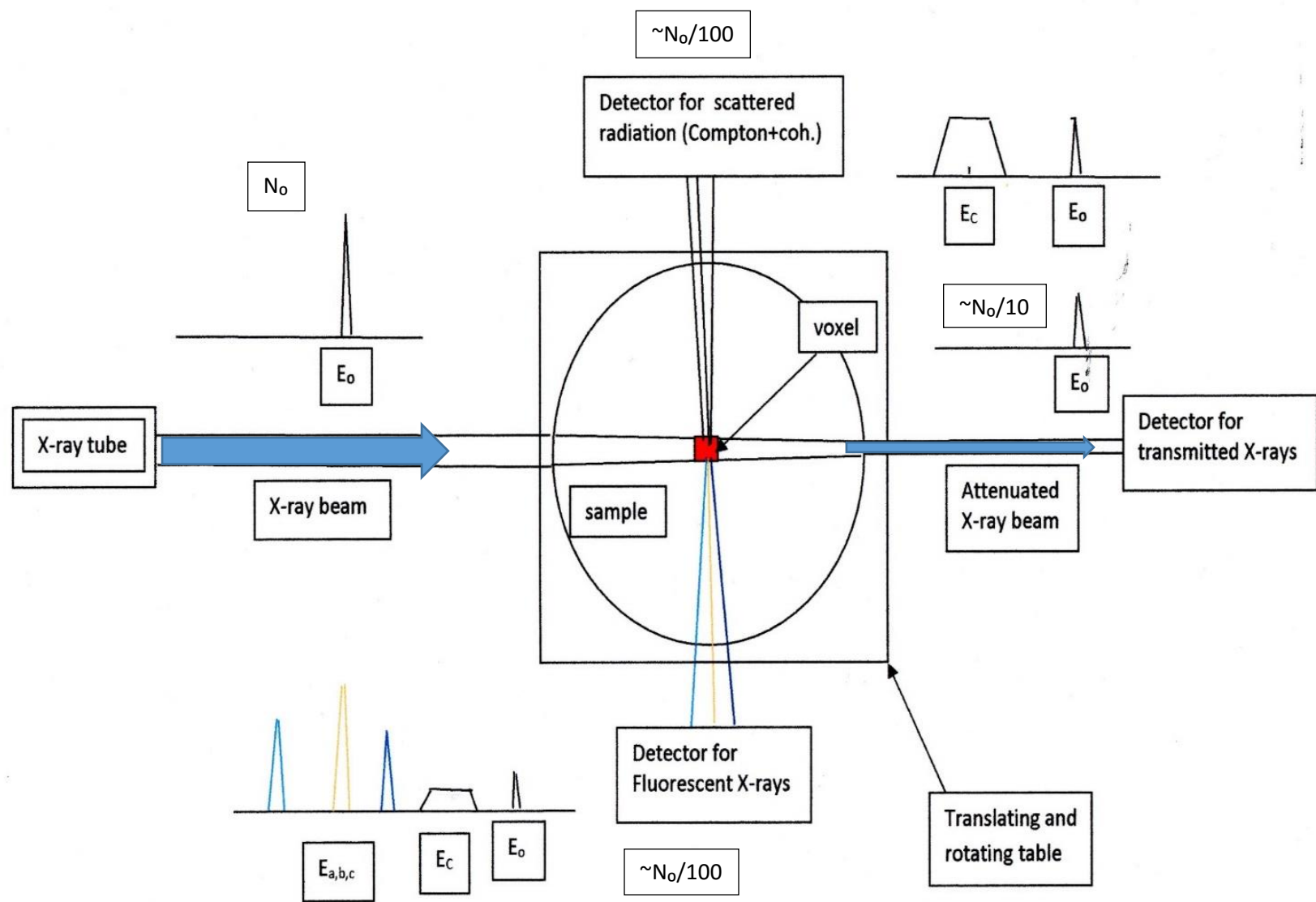
- **W.C. Röntgen 1901**
- **Max von Laue 1914**
- **W.H. Bragg and W.L.Bragg 1915**
- **C.G.Barkla 1917**
- **K.M.G. Siegbahn 1924**
- **A.H. Compton 1927**
- **P.J.Debye 1936**
- **D.Hodgkin 1964**
- **A.M.Cormack and G.H. Hounsfield 1979 (50 years ago!!)**

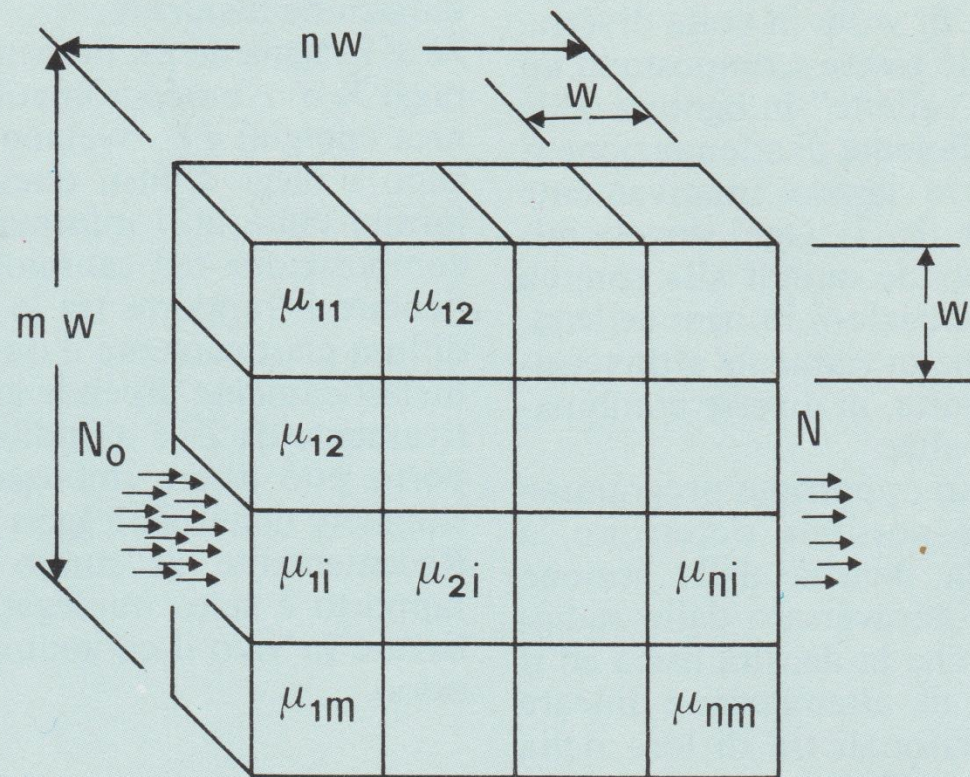
PRINCIPLES OF X-RAY TOMOGRAPHY:
COLLIMATED X-RAY BEAM AND A LARGE
NUMBER OF ATTENUATION MEASUREMENTS
CROSSING THE OBJECT AT ALL POSSIBLE
POSITIONS AND ANGLES.

- With the word “tomography” is intended a method in which an incident collimated photon beam is **transmitted** through an object to be studied ; this object is translated and rotated, in such a manner that a complete volume (section x height of the beam) is irradiated. A large number of attenuation measurements are , therefore, carried out. With a mathematical procedure, the irradiated section of the object is “reconstructed” approximately to the density map and to the atomic number Z .

- **PHYSICAL BASIS FOR X-RAY TOMOGRAPHY**
- **(the name tomography derives from the greek: tomos = layer e graphos=to write)**
-
- **$N = N_0 e^{-\mu x}$ attenuation of monoenergetic X or gamma-rays by**
- **an homogeneous object**
- **$N = N_0 e^{-\sum \mu(i) \Delta x}$ attenuation of monoenergetic X or gamma-rays**
- **by an inhomogeneous object**
- **$N = N_0 e^{-\int \mu(s) ds}$ tomography, through mathematical**
- **reconstruction of the image**
- **(transformada de Radon – Johann Radon 1917)**
- **μ = linear attenuation coefficient depending on physical density and atomic number**







$$\mu_{1i} + \mu_{2i} + \cdots \mu_{ni} = \frac{1}{w} \ln \frac{N_o}{N}$$

1979 : **NOBEL PRIZE FOR MEDICINE** TO:
ALLAN MCLEOD CORMACK : South African
Physicist and
GODFREY H. HOUNSFIELD : British electronic
Engineer.

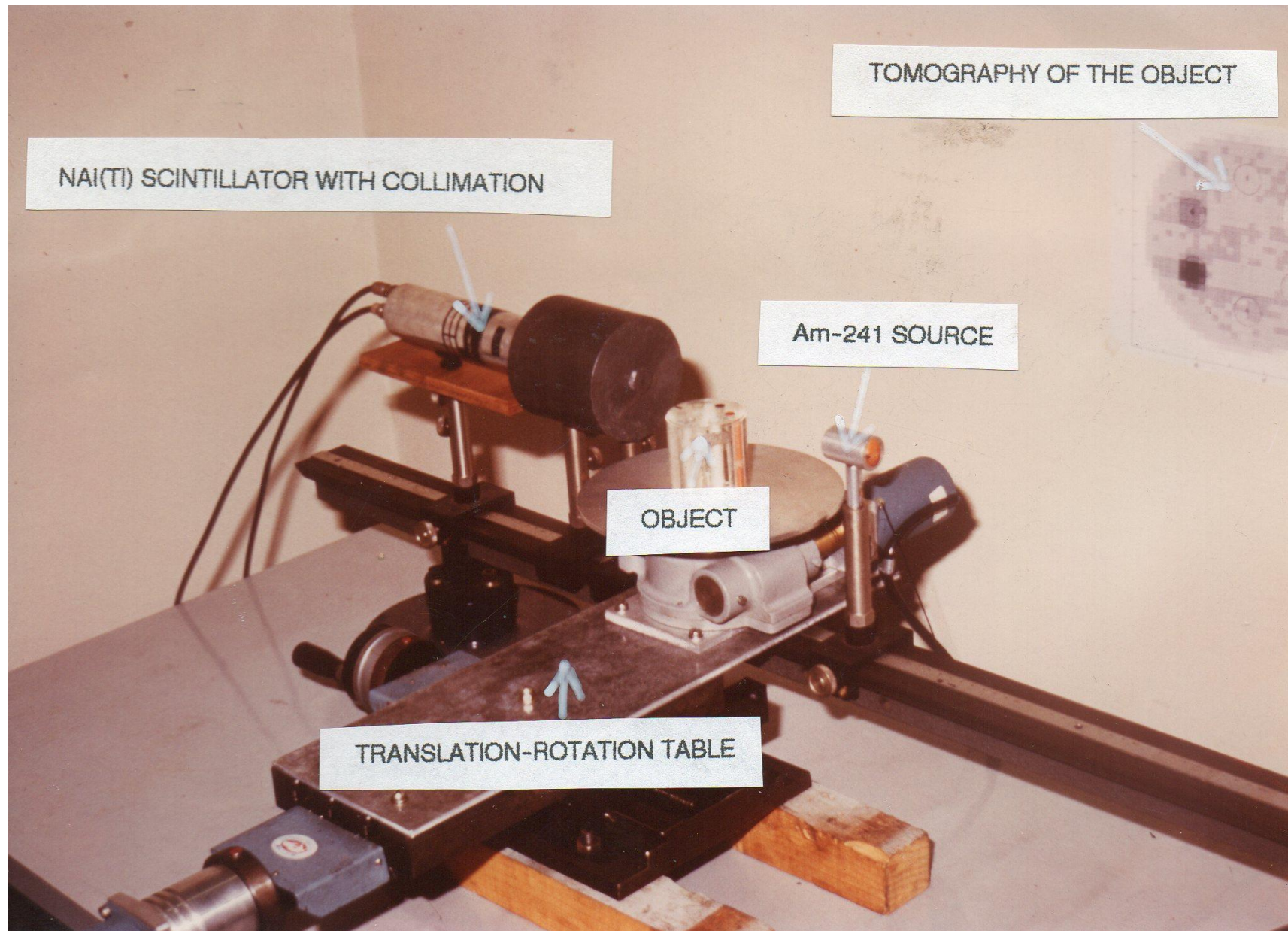
NAI(Tl) SCINTILLATOR WITH COLLIMATION

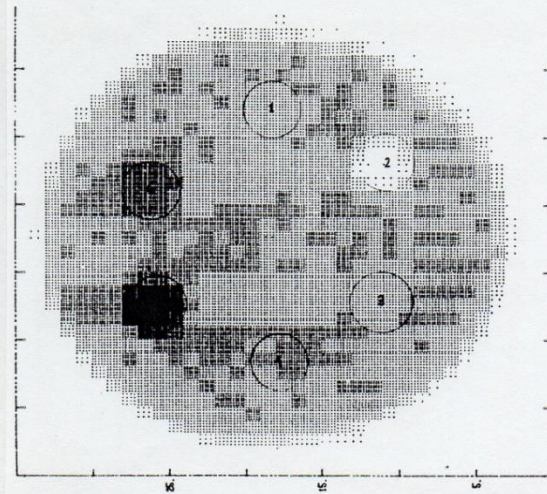
TOMOGRAPHY OF THE OBJECT

Am-241 SOURCE

OBJECT

TRANSLATION-ROTATION TABLE

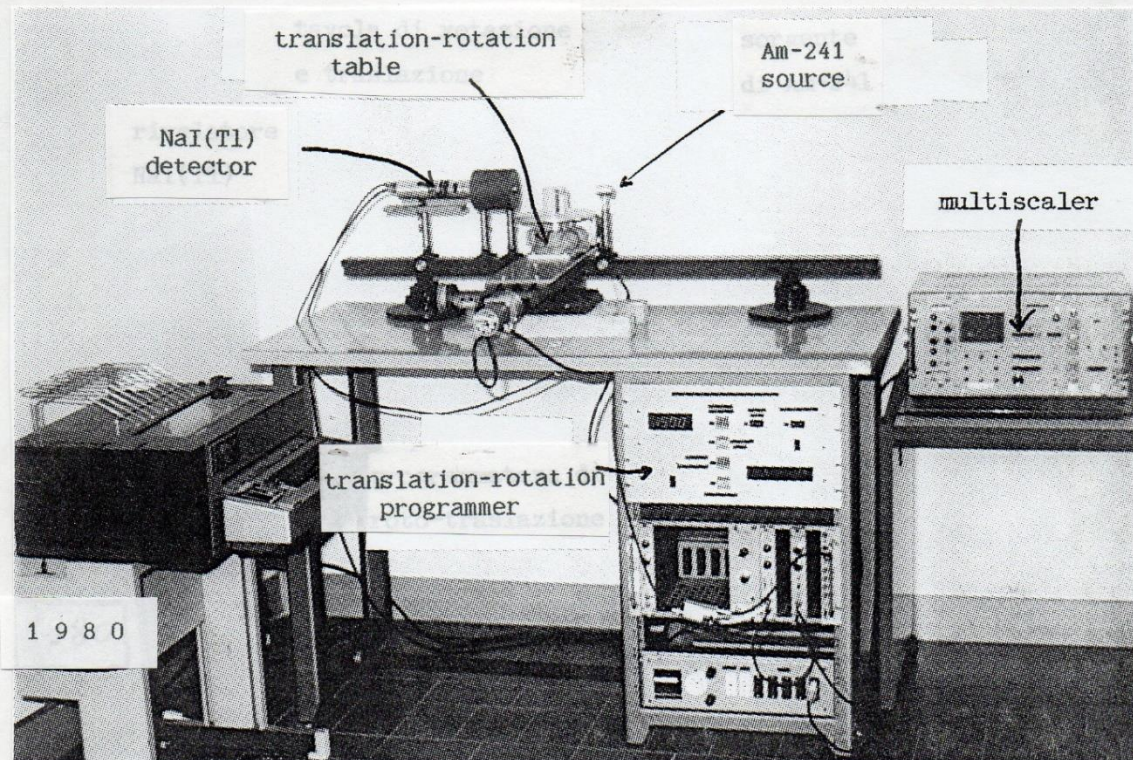




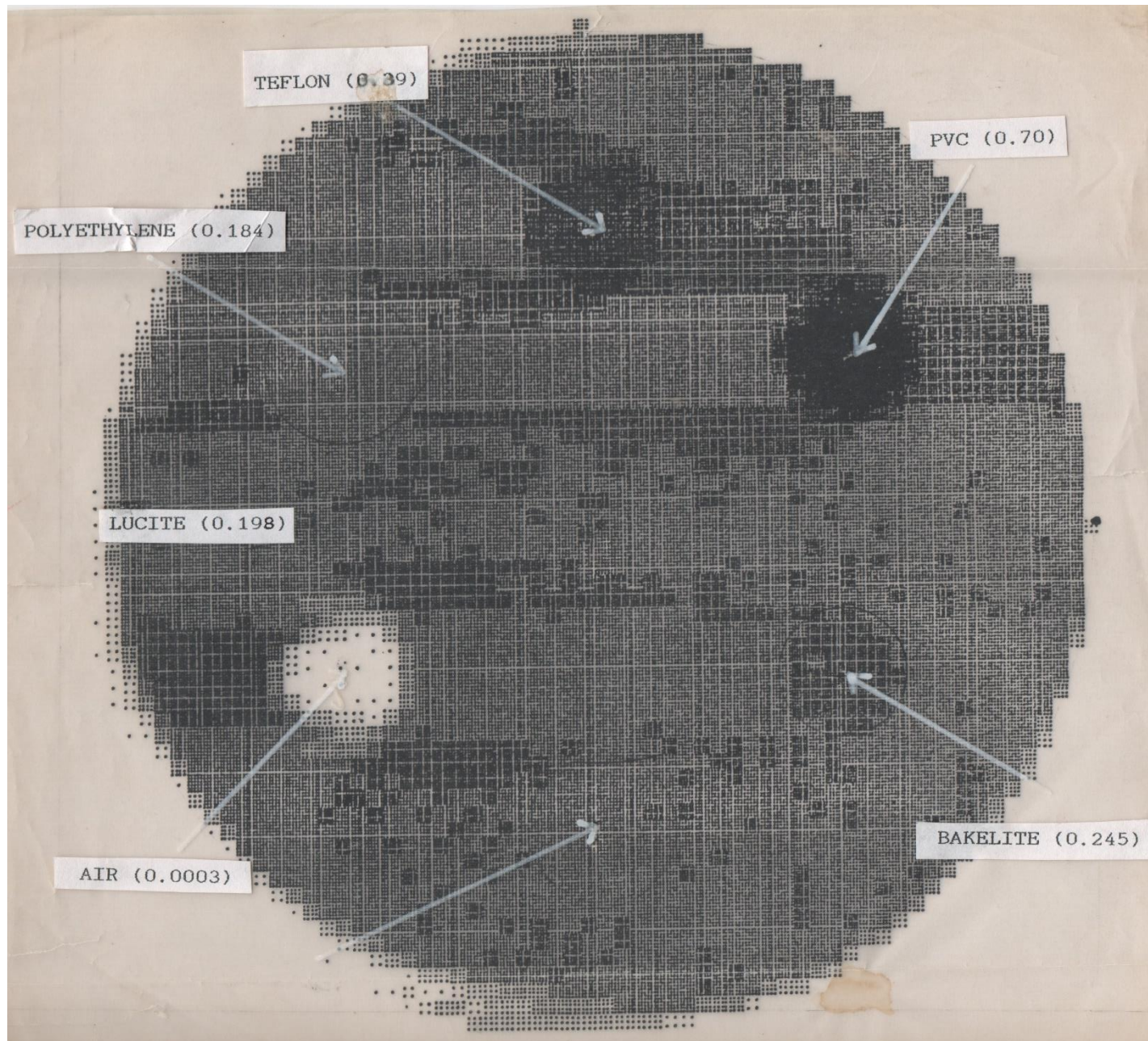
linear attenuation coefficient (cm^{-1})

from tomography theoretical

1. polyeth.	0.188	0.184
2. air	0	0
3. nylon	0.21	0.216
4. bakelite	0.23	0.245
5. PVC	0.71	0.70
6. teflon	0.35	0.39



1980



USING A COMPUTED TOMOGRAPHY MINISCANNER IN SOIL SCIENCE

S. CRESTANA,¹ R. CESAREO,² AND S. MASCARENHAS¹

In a previous paper (Crestana et al. 1985) we demonstrated the possibility of using computed tomographic (CT) scanning for investigations in soil science. One of the main limitations was the complexity and high cost of medical CT scanners. In this paper we report on the characteristics and use of a very inexpensive, homemade CT miniscanner dedicated to soil science analysis. This new apparatus was applied to carrying out tomographies of soil with various water contents and also to obtaining the best conditions and adequate physical parameters for optimized attenuation measurements in soil. Our results demonstrate that it is now possible to have a CT miniscanner, without the limitations of the medical CT scanner, that should be invaluable for advanced studies in soil science.

N_{AV} is Avogadro's number, Z and A are the atomic number and the atomic weight, respectively, of elements constituting the sample, and δ is the physical density.

Except for materials containing hydrogen, the electronic density δ_e is with good approximation proportional to the physical density.

The situation is not very different for analyzing soil samples. For soils the contribution of the Compton effect is approximately 80% at 80 keV, the remaining contribution being mainly due to the photoelectric effect. Therefore, a tomographic map of soil at 60 to 100 keV is to a first approximation proportional to the distribution of the physical density, while a tomographic map at lower energy (20 to 30 keV) would be mainly proportional to a high power of the atomic number Z (photoelectric effect).



With Silvio Crestana and Juca Cruvinel, who carried out the first CT-scanner for soil tomography in Sao Carlos, in 1985.

- **1990 : TOMOGRAFO INDUSTRIAL COM A GILARDONI**



Tomography of a tree carried out “in vitro” ; the sequence of annual rings is clearly visible. This tomography can be also carried out “in vivo”

- **MICRO- TOMOGRAPHY**
- **Micro-tomography simply indicates that the incident beam, from an X-ray tube or from synchrotron radiation, is strongly collimated. The level of collimation mainly depends on the beam intensity, because more collimation is related to less photons.**



UNIVERSITÀ DEGLI STUDI DI ROMA
"LA SAPIENZA"

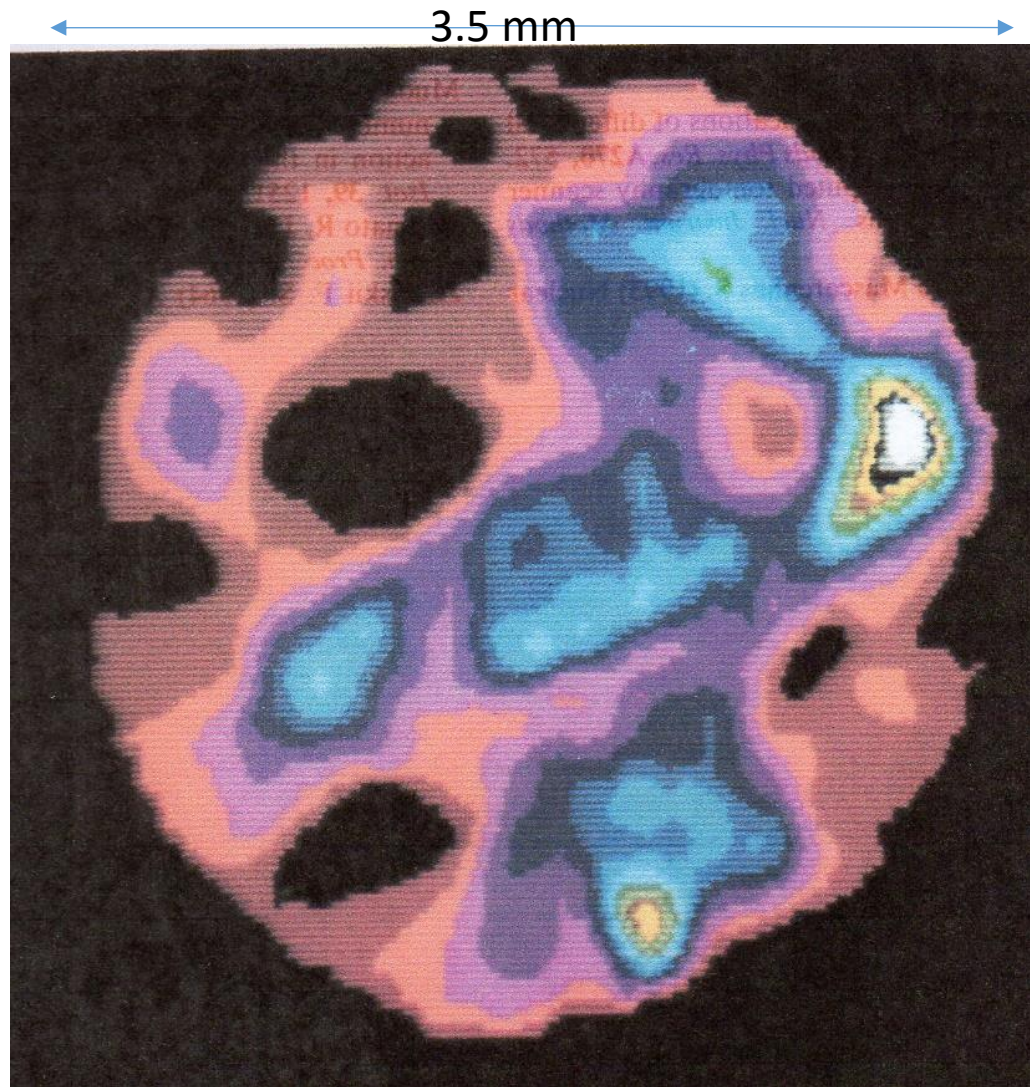
CENTRO INTERDIPARTIMENTALE
DI RICERCA PER L'ANALISI DEI
MODELLI E DELL'INFORMAZIONE
NEI SISTEMI BIOMEDICI
CISB

C.R. APPOLONI R. CESAREO

MICROSCANNING AND MICROTOMOGRAPHY WITH X-RAY TUBES

RAP. 04.94

DICEMBRE 1994



**GRAINS OF SOIL with
CARLOS R. APPOLONI , UNIVERSIDADE DE LONDRINA**

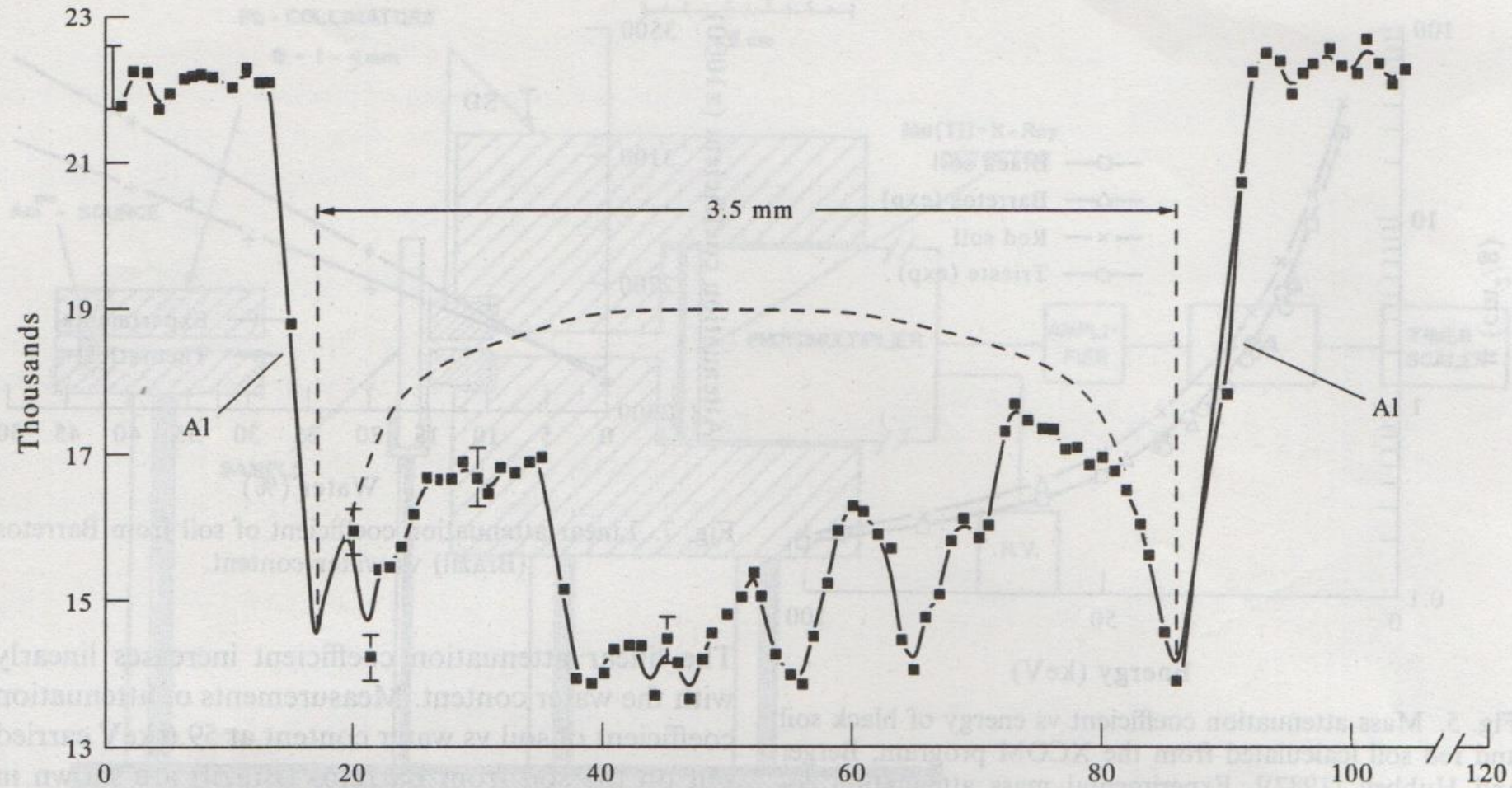
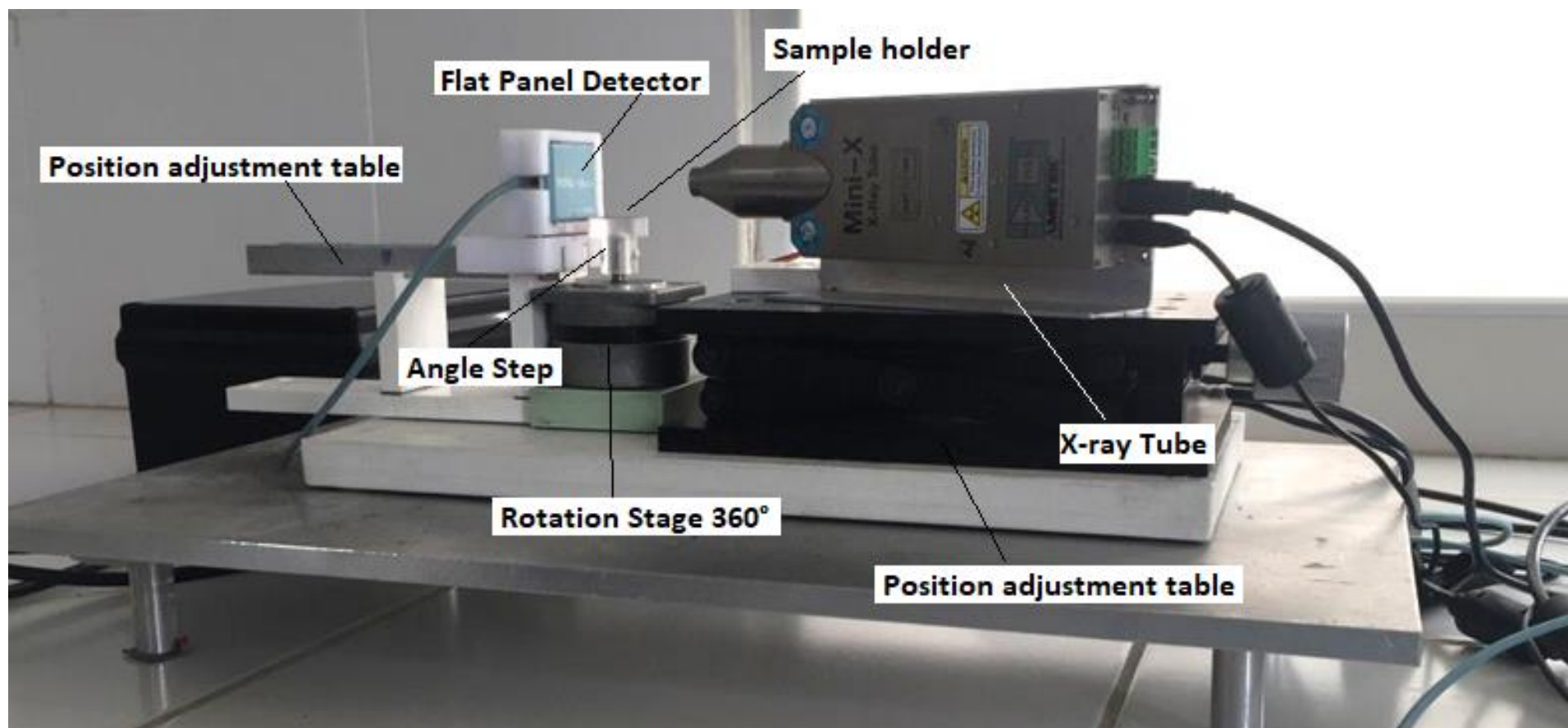
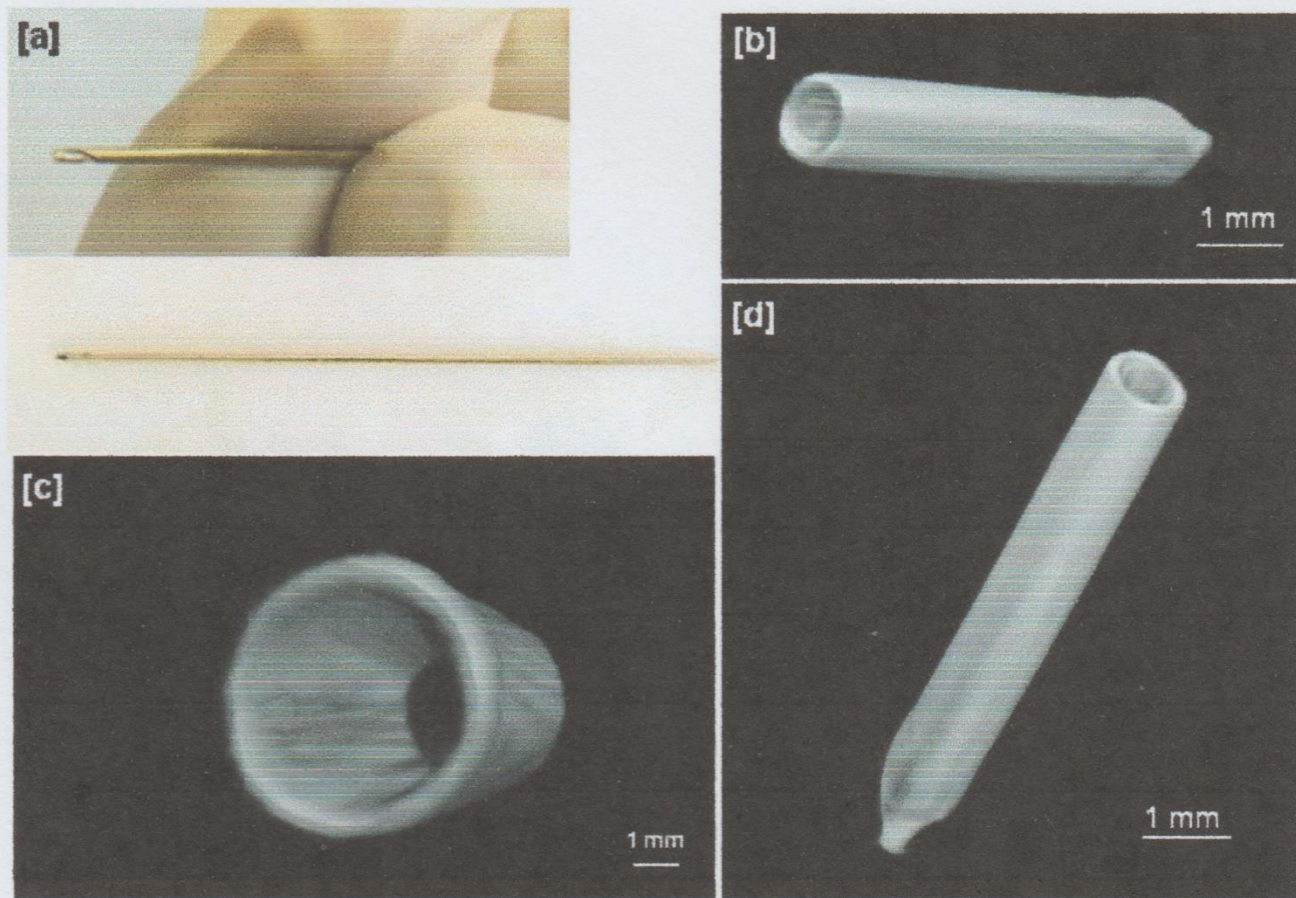


Fig. 8. Scan of an aluminium cylinder, with an i.d. of 3.5 mm, filled with soil grains. The dotted curve refers to the Al cylinder without anything at the interior. The effect of the grains (4–5) is evident.







Figur 4.50- Photo (top left) and micro tomographic images of needle PACEB-F4-00082. The needle is void, and the gold thickness is 150 μm approximately.

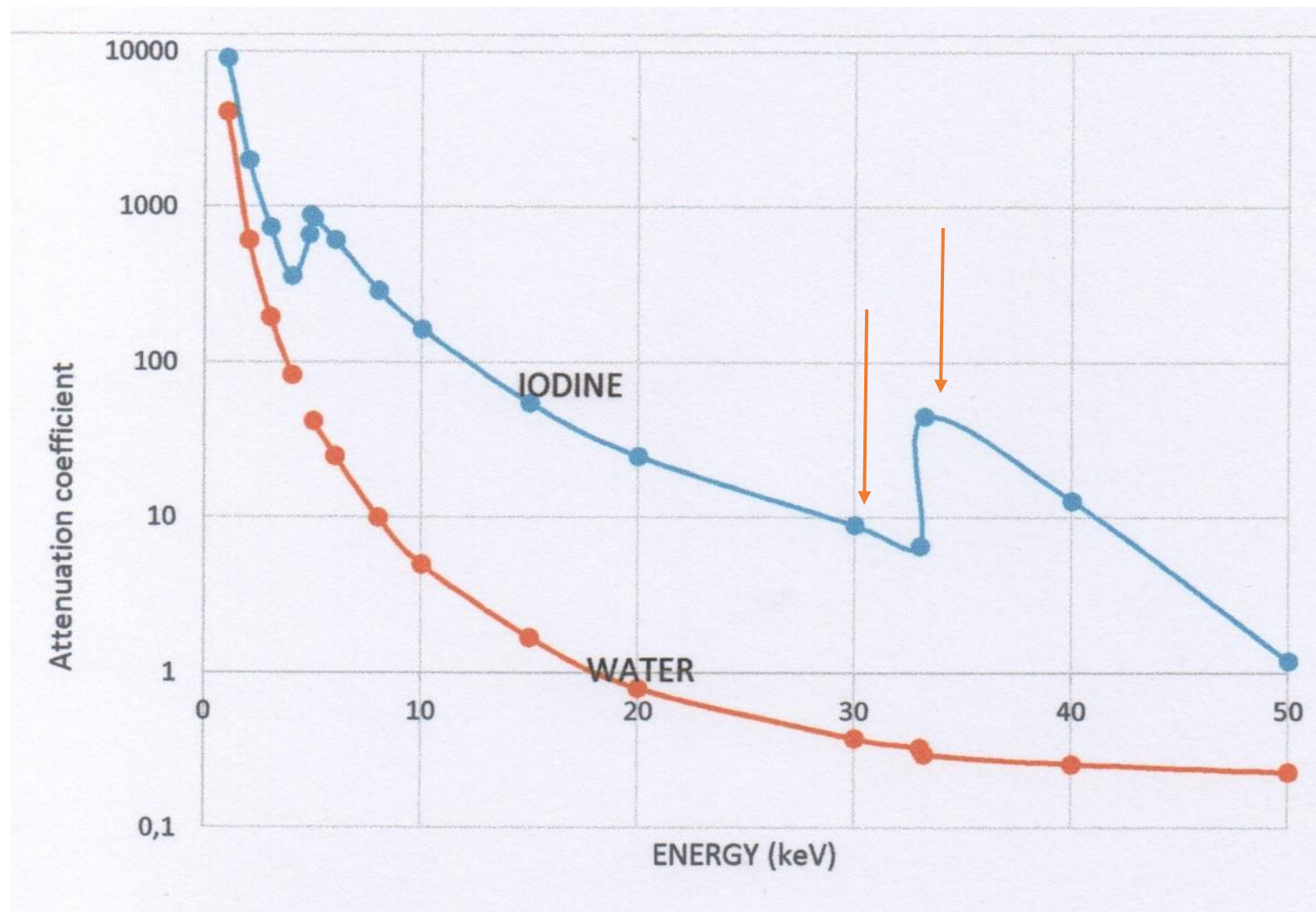
Soraia Azeredo & Ricardo T. Lopes COPPE, UNIVERSIDADE FEDERAL DO RIO DE JANEIRO

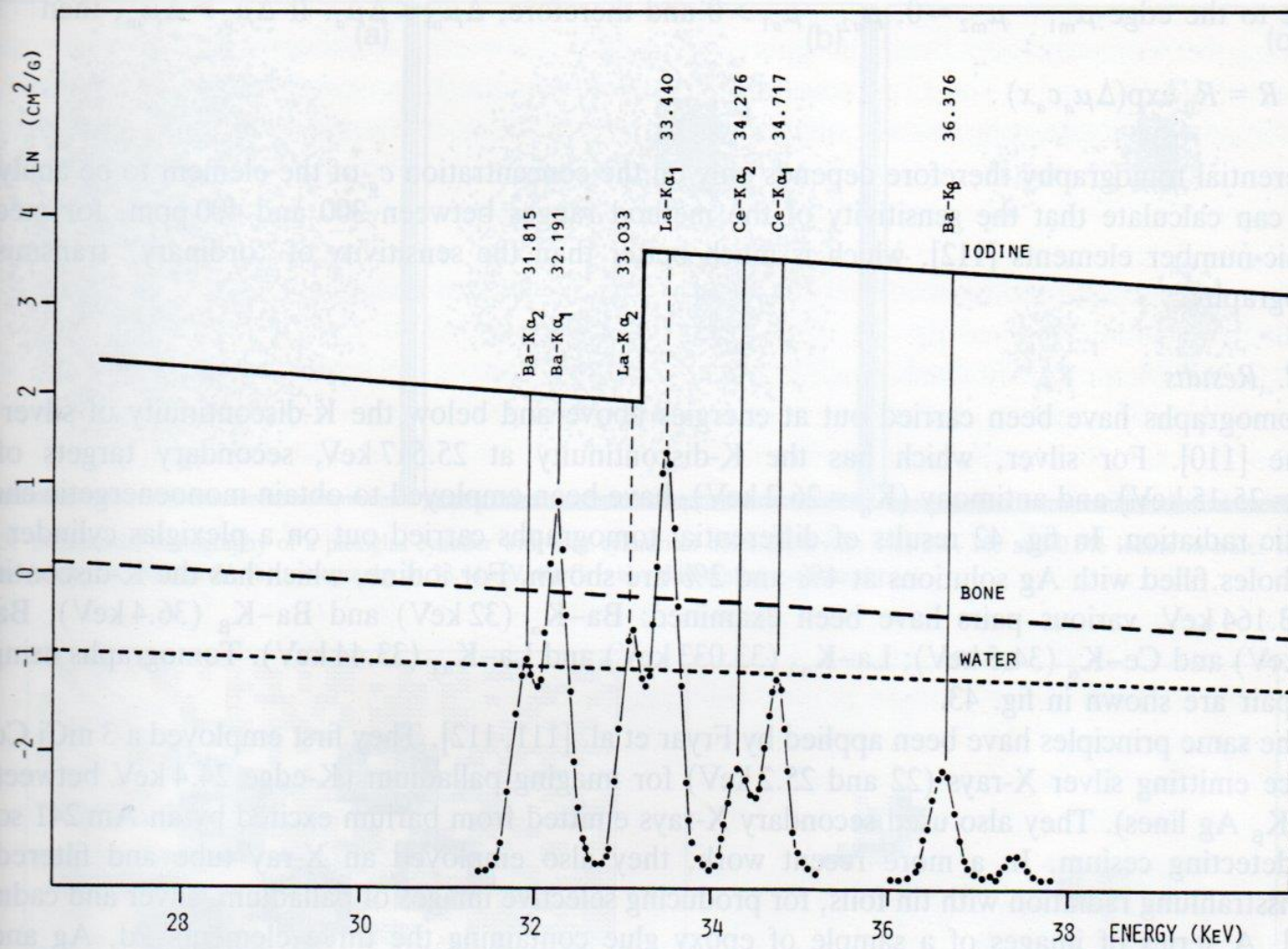


**Angel Bustamante (Universidad Nacional de San Marcos, Lima, PERU) and Soraia Azeredo (COPPE, Universidade Federal do Rio de Janeiro) .
In the middle the micro-CT scanner.**

- **ALTERNATIVE TOMOGRAPHIC METHODS**
- **DIFFERENTIAL TOMOGRAPHY AND MARKERS**
- Attenuation coefficient μ of all elements show a sharp discontinuity due to discontinuity of the photoelectric effect (maximum of μ at the minimum energy to eject an electron from the internal shells , K, L ...) .
- For example iodine, typical contrast medium for the human body, has its K-discontinuity at 32.3 keV. The difference between two tomographs carried out at two energies close below and close to above 32.3 keV , will be able to amplify the presence of iodine. For example secondary targets of Lanthanum and Barium emits $K\alpha$ -rays with energy 33.4 and 33 keV ($K\alpha_1$ and $K\alpha_2$) and 32.2 and 31.8 keV ($K\alpha_1$ and $K\alpha_2$) respectively.

The method of differential tomography, by monochromatizing the bremsstrahlung output of an X-ray tube with secondary targets and by scanning a sample at two energies, above and below the energy of the photoelectric discontinuity of the element to be visualized was employed to study the absorption of tracers by plant (using a iodine solution) and animals (using a Gd-DTPA complex).





1. Attenuation coefficient of iodine, showing the K-discontinuity, and position of the energy values of X-rays of barium, lanthanum and cerium, useful for the differential tomography of iodine.

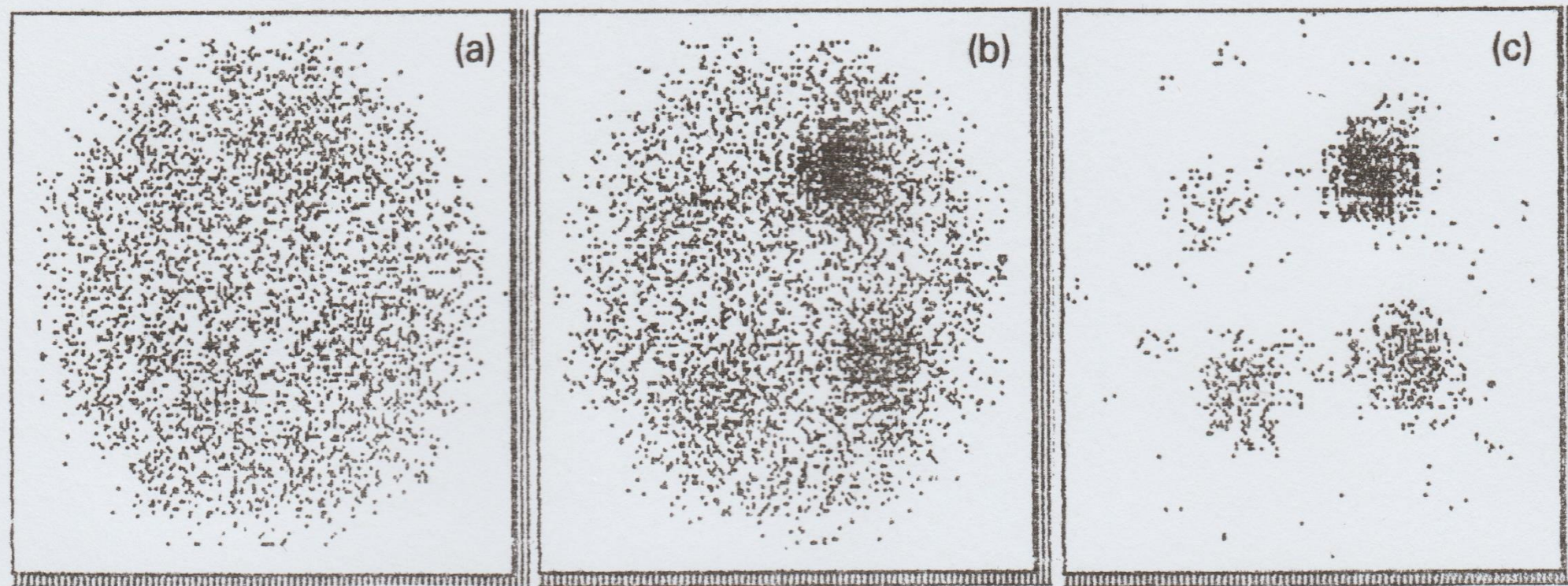


Fig. 43. Differential tomography of a plexiglas cylinder with four cylindrical holes filled with 4%, 2%, 1% and 0.5% iodine in water solution. (a) tomography at 33.033 keV, (b) tomography at 33.44 keV, (c) $(b - a)$ = differential tomography.

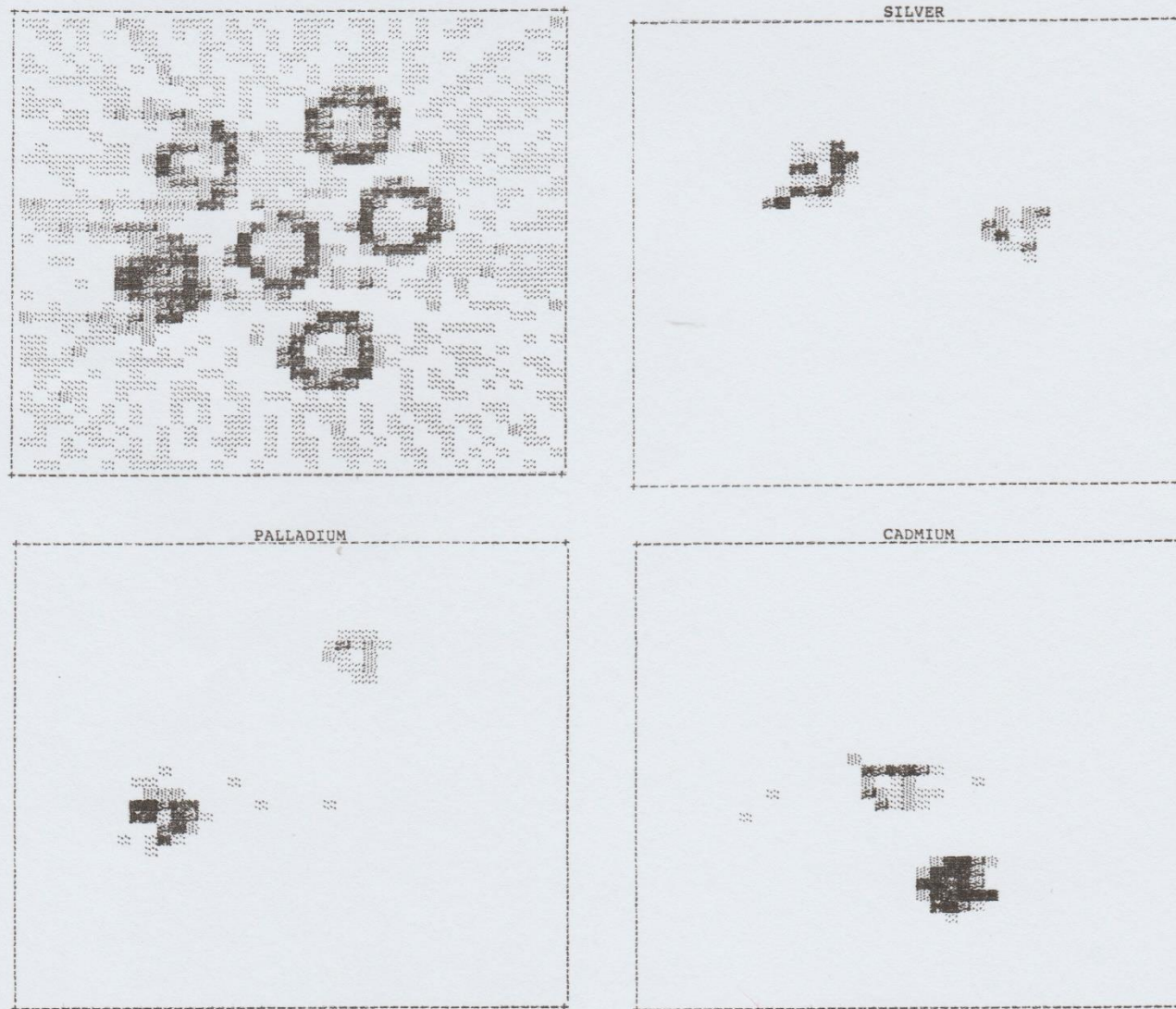
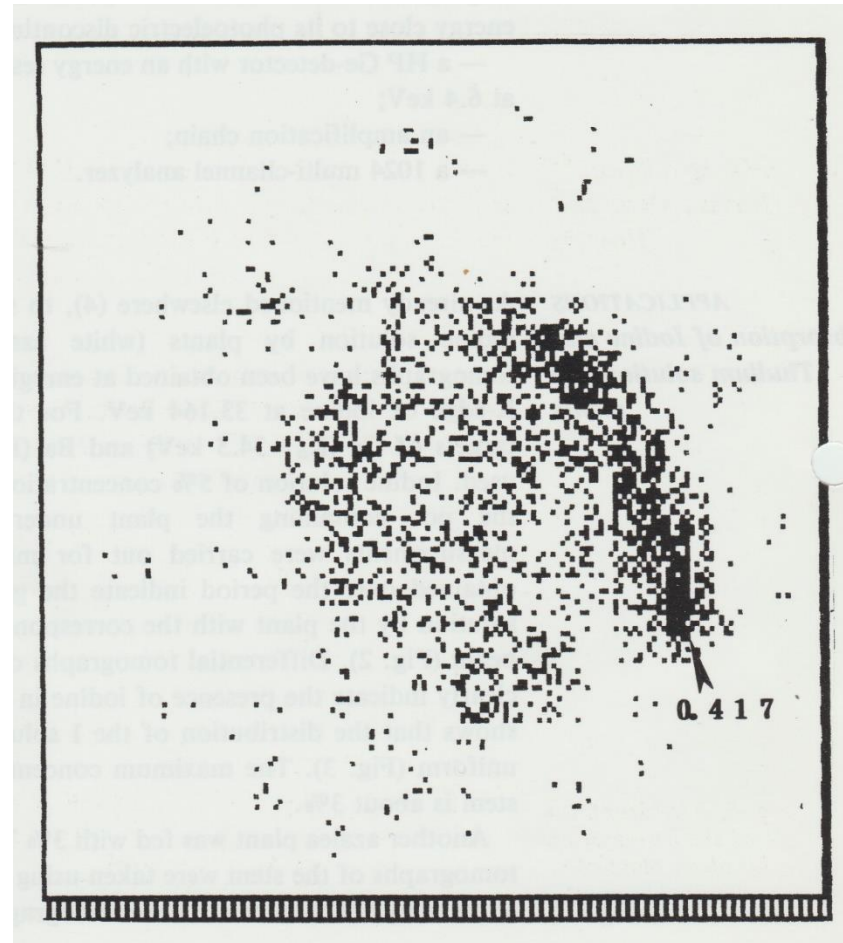
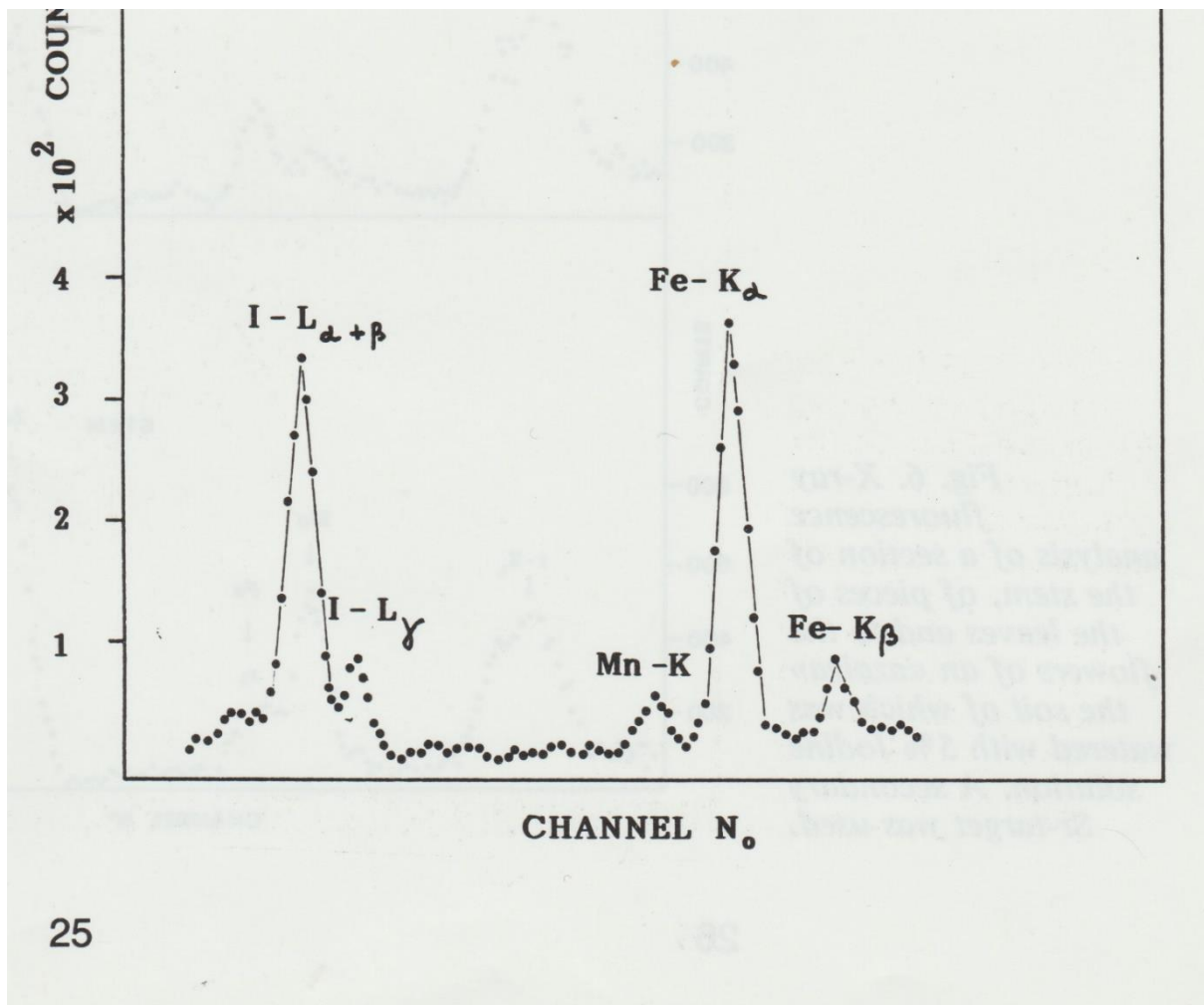


Fig. 44. Upper left: "normal" tomography of the test object containing Pd, Ag and Cd. Lowe left: differential tomography of Pd. Upper right: differential tomography of Ag. Lower right: differential tomography of Cd.

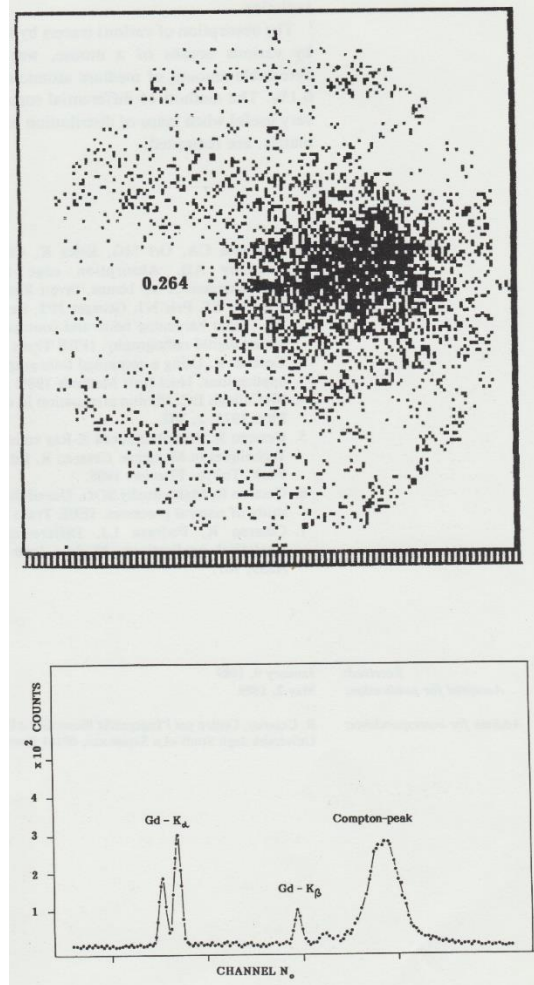


Differential tomography showing the uptake and selective distribution of iodine solution in the stem of an Azalea plant.



25

XRF-spectrum of the leaves of an azalea after absorption of Iodine solution



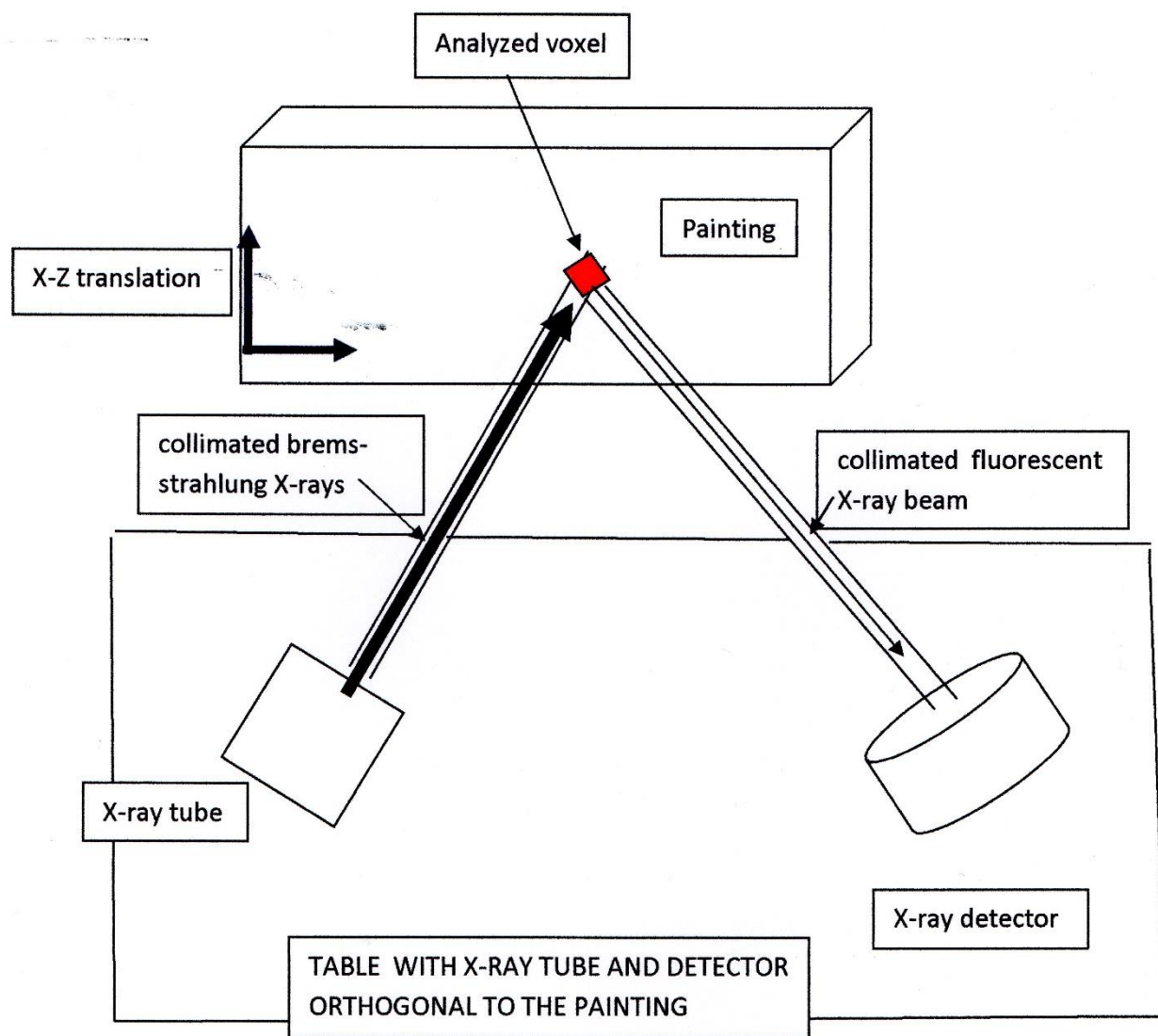
Gadolinium distribution and XRF-spectrum in the kidney of a mouse

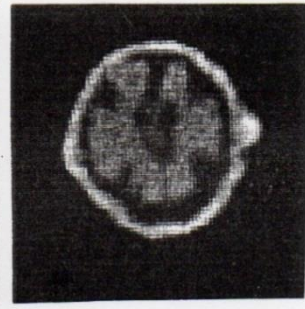
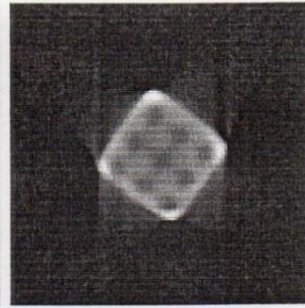
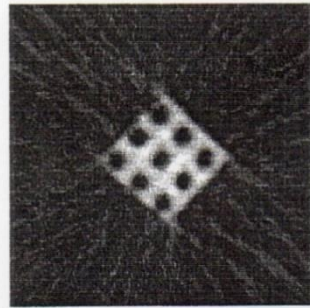
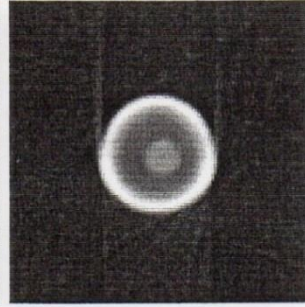
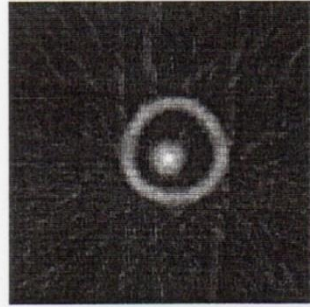
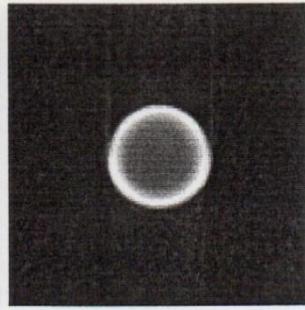
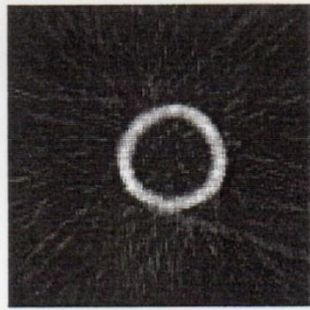
- **As another example, silver has the photoelectric discontinuity for the most interne orbit (K) at an energy of 25 keV. The difference of two tomographs, carried out at energies below and above the discontinuity of this element (using for example tin and antimony secondary targets, which emit 25.15 keV and 26.2 keV as $K\alpha$ -lines) will enhance its presence .**

- Besides the transmitted photons, also scattered photons (for example Compton photons scattered at 90°) can be analyzed for each transmission measurement, and, with a similar procedure, the irradiated section can be reconstructed. It can be demonstrated that the map of the photons scattered by a single elemental volume is proportional to the physical density.
- Also secondary photons emitted through photoelectric effect by a volume element can be employed (secondary X-rays), which intensity is depending on the atomic number and concentration of the specific element. A map is obtained, which gives the distribution of this element in the irradiated volume.

- **COMPTON TOMOGRAPHY**

- Compton tomography simply uses the Compton scattered photons, generally at 90° , instead of the transmitted photons (not because of the intensity to image the section of an object).





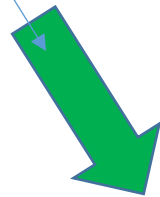
- COMPTON TOMOGRAPHY : 2002
- BRUNETTI, CESAREO ET AL. CORK (CORTIÇA)
QUALITY ESTIMATION

NO TRANSMITTED PHOTONS



WALL

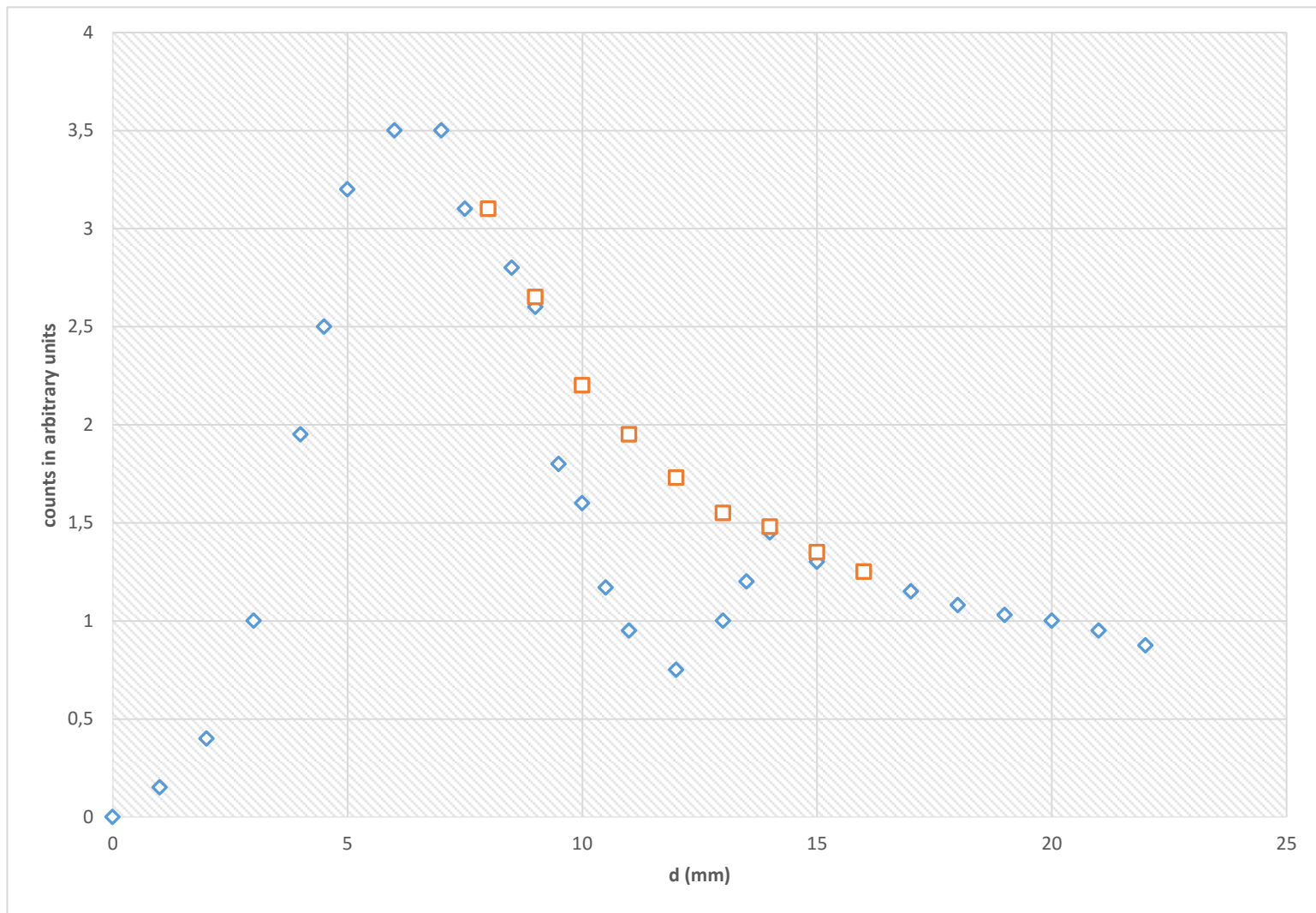
X-RAY SOURCE

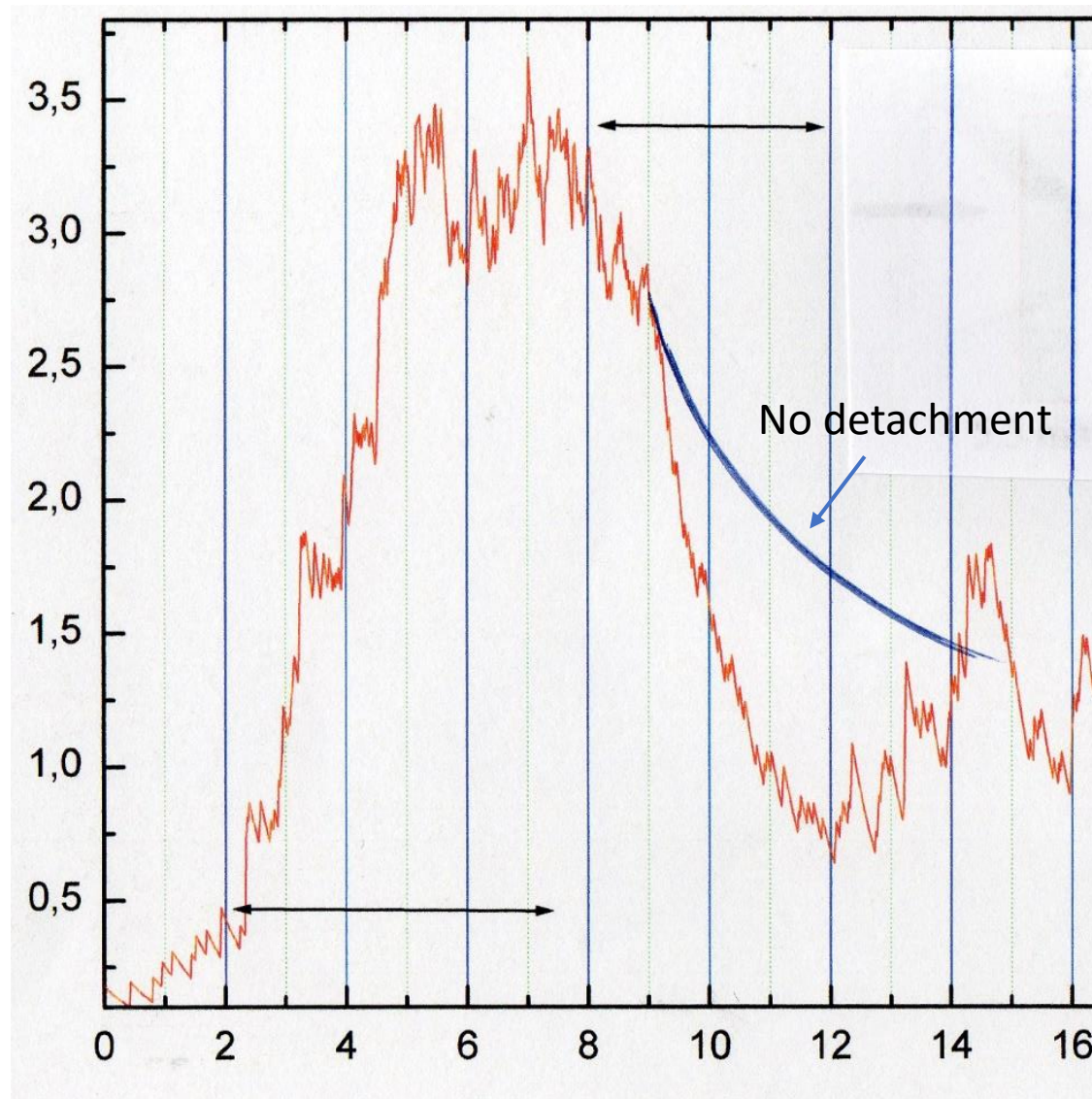


COMPTON SCATTERED PHOTONS

APPLICATION OF COMPTON TOMOGRAPHY TO EVALUATE THE DETACHMENT OF A FRESCO
BY RAPHAEL IN THE VATICAN MUSEUM (STANZA DI ELEODORO)







COMPTON SCATTERING AND FRESCO DETACHMENT

- **X-RAY FLUORESCENCE TOMOGRAPHY (XRF-SCANNING)**
- In this case, the photons are analyzed, emitted by fluorescence effect by the chemical elements present in the sample. This method is effective when the emitted X-rays have sufficient energy according to size and composition of the sample to be analyzed, i.e. from $Z \sim 20$ (calcium) to $Z \sim 53$ (iodine) for K-lines and from $Z \sim 53$ to $Z = 92$ for L-lines.

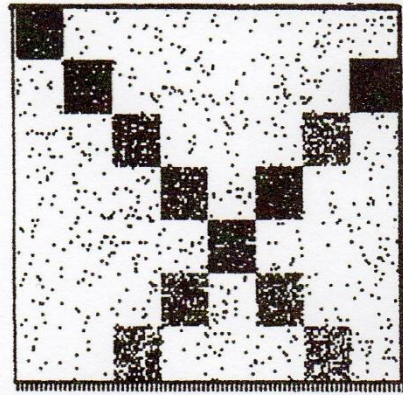


Fig. 52. XRF tomography of a test object on plexiglas, with holes on the diagonal, filled with a solution containing 0.5% iodine.

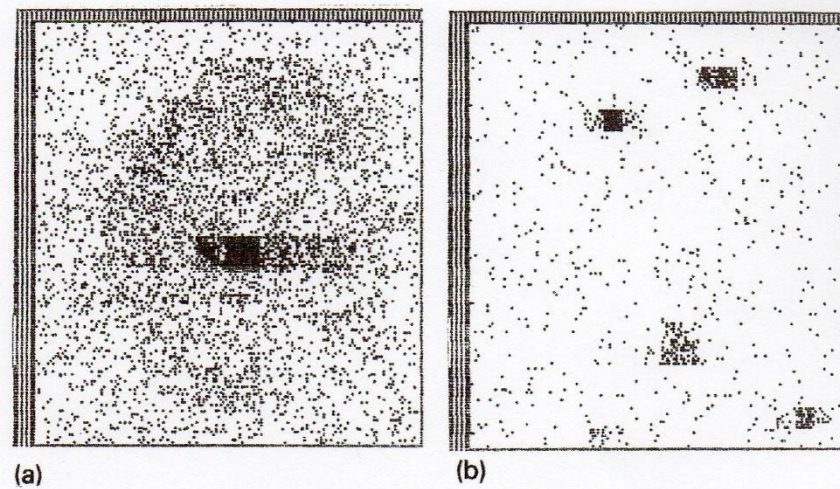
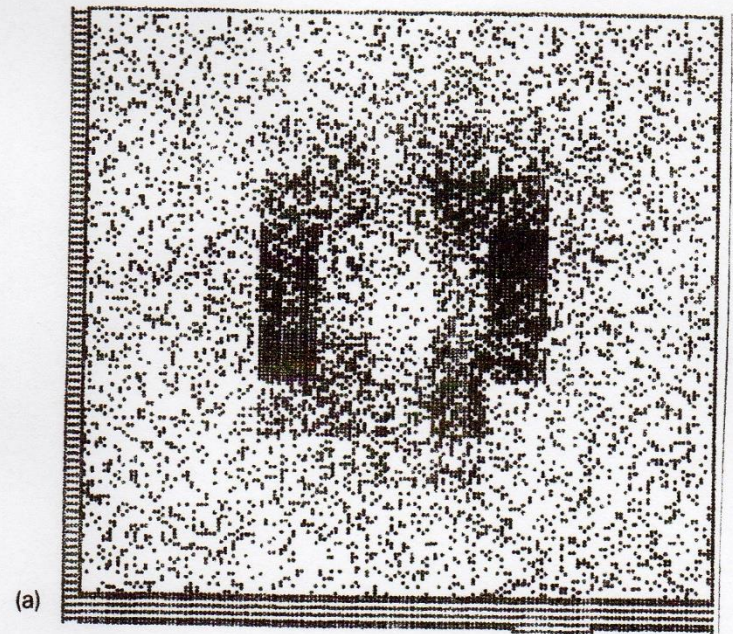


Fig. 53. (a) XRF tomography of an object containing epoxy resins mixed with a Ag grain (in the middle). The scanned surface is about 6×6 mm². (b) XRF tomography of a plexiglas object containing Cu wires disposed vertically. The scanned section is about 8×8 mm².



(a)

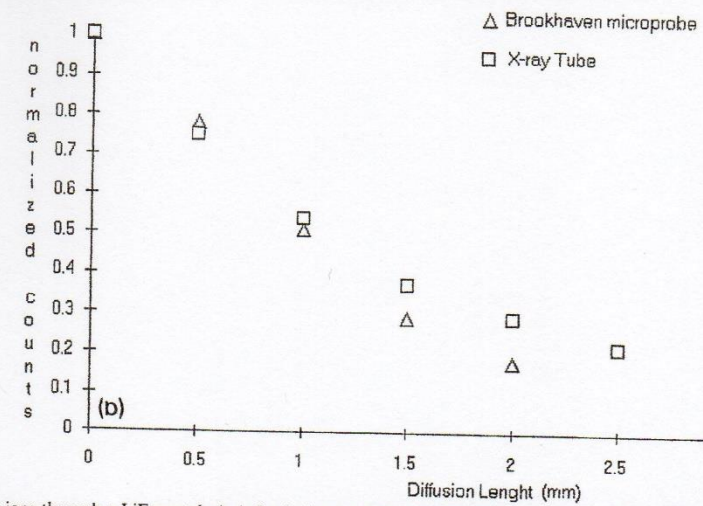


Fig. 54. (a) Diffusion of Ag ions through a LiF crystal. A AgI solution was put into a cylindrical hole drilled in the center of the crystal, which was then heated at 600°C for 24 h. The solution was then removed from the hole, and the Ag content measured in a section of the crystal orthogonal to the drilled cylinder, by means of the fluorescence X-ray tomography. (b) Ag content along a diagonal line of the section described in a), determined with an X-ray tube (□) and with synchrotron radiation (Δ).



Roberto Cesareo and Sergio Mascarenhas in Rome around 1985, at the Laboratory of the “Centro per l’ingegneria biomedica”



New tomographic methods using X-ray tubes

R. Cesareo

Centro per l'Ingegneria Biomedica, Università di Roma "La Sapienza", Rome, Italy

S. Mascarenhas and S. Crestana

EMBRAPA/NPDIA and Institute of Chemistry and Physics, University São Paulo, S. Carlos, SP, 13560, Brazil

A. Castellano

Dipartimento di Scienze dei Materiali, Università di Lecce, Lecce, Italy

Different kinds of images of the section of a sample can be deduced from the interaction of X-rays with matter:

(1) When two X-ray beams are employed, the energies of which closely bracket a photoelectric discontinuity of a sample, then the difference of two images carried out with the pair of X-rays is only sensitive to the element whose tomography, called "differential tomography", gives the distribution of the element in the section.

(2) Fluorescent X-rays emitted by the voxel identified by the intersection of the collimated incident beam with secondary beam can be mapped versus the $x-y$ position of the voxel: an image can be obtained (called XRF-tomography) showing the distribution of all fluorescent elements.

(3) When the diameter of the beam in the transmission tomography is reduced to the order of magnitude of "microtomography" is obtained, in which the geometrical resolution is of the same order of magnitude.

A NEW TOMOGRAPHIC DEVICE BASED ON THE DETECTION OF FLUORESCENT X-RAYS

Roberto CESAREO¹⁾ and Sergio MASCARENHAS²⁾

¹⁾ Dipartimento di Energetica and Centro per l'Ingegneria Biomedica, Università di Roma "La Sapienza", Corso Vittorio Emanuele II, 244, 00186 Rome, Italy

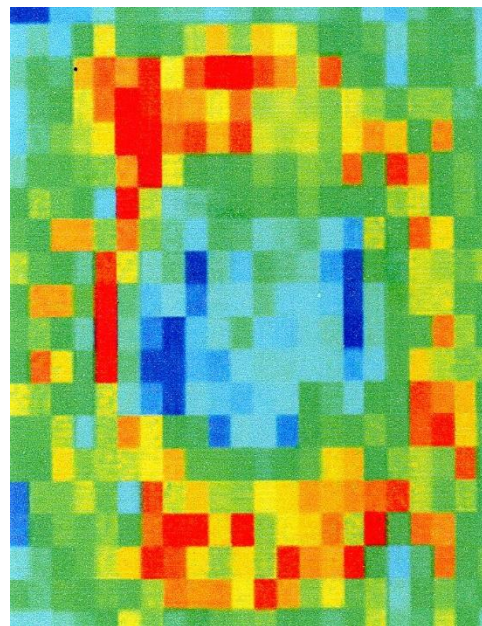
²⁾ UAPDIA-EMBRAPA, S. Carlos, S.P. 13560, Brazil and
Institute of Physics and Chemistry, University S. Paulo, S. Carlos, S.P. 13560, Brazil

Received 1 November 1988

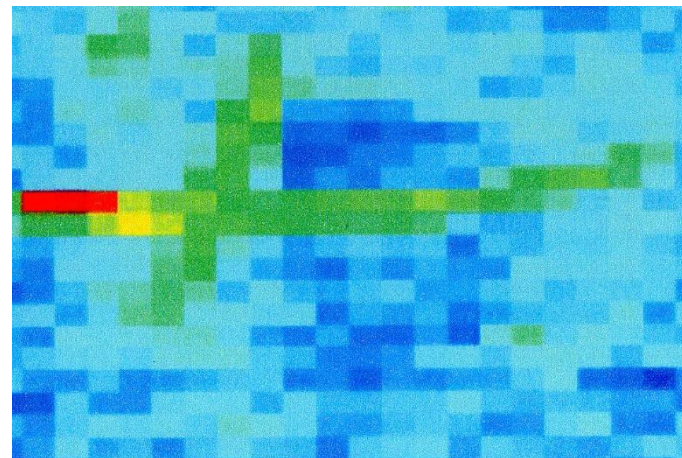
Fluorescent X-rays emitted by a small volume (voxel) of an irradiated sample can be employed for obtaining tomographic images. A finely collimated beam from an X-ray tube has been employed, and the X-rays emitted at 90° by the elements in a voxel have been analyzed with a highly collimated detector. Moving the sample in the $x-y$ plane, the elemental distribution can be determined in the slice of the object crossed by the radiation. The intensities of the measured peaks have been corrected for absorption effects in the object. The distribution of iodine in test objects has been determined.



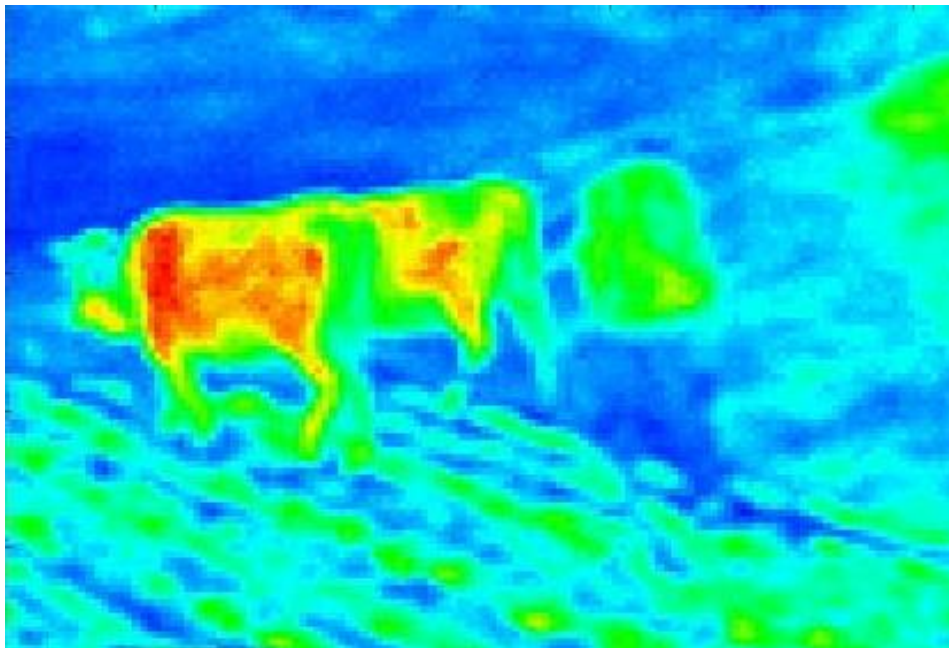
STAMP FROM CHILE



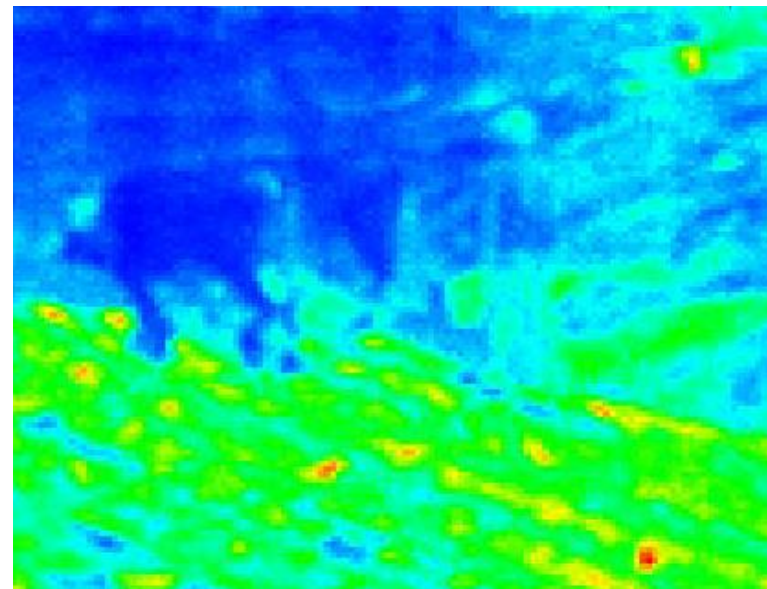
MERCURY



IRON



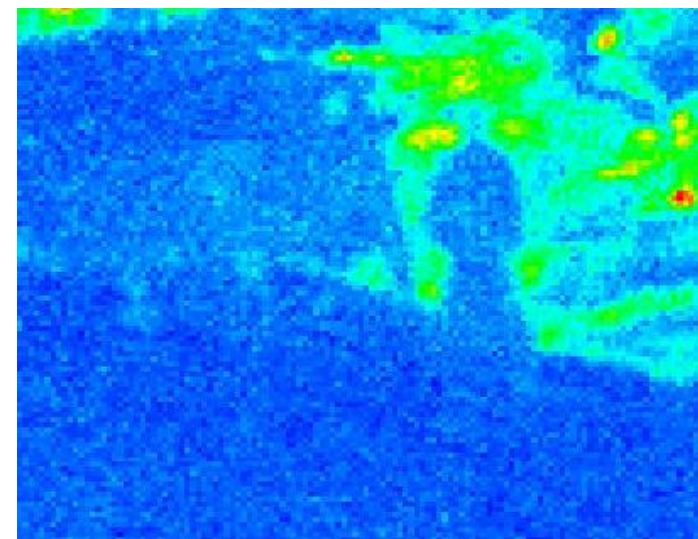
Zinc K alfa



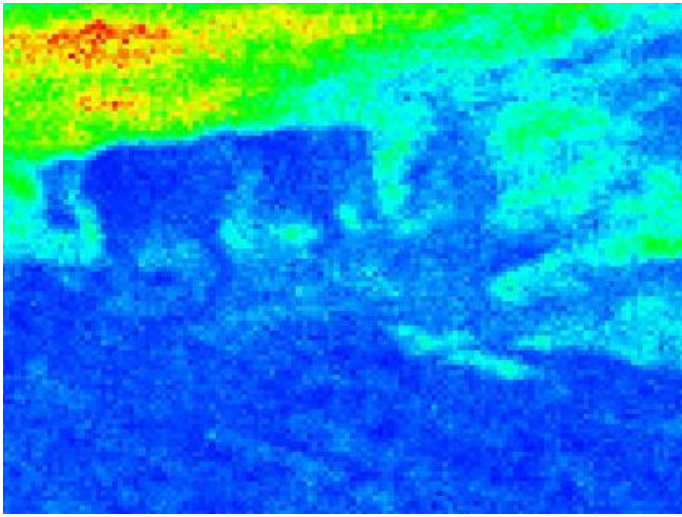
Iron K alfa



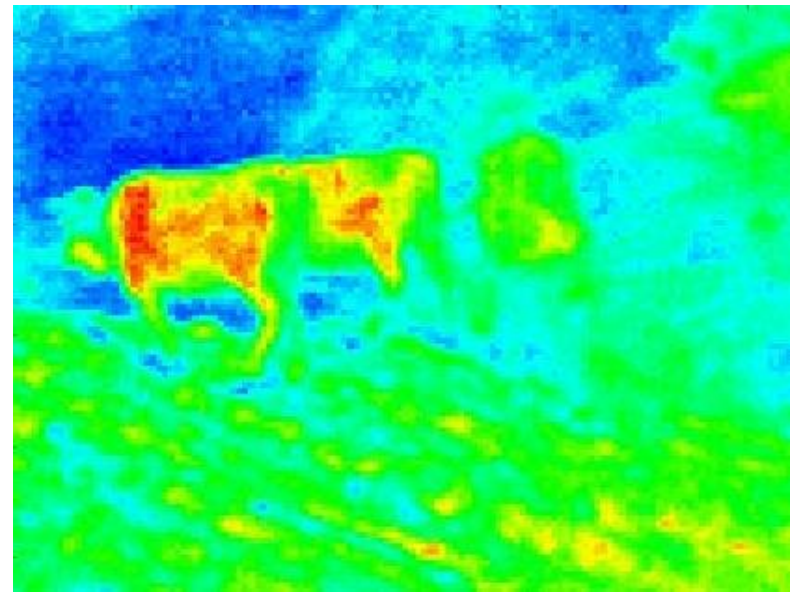
Visible



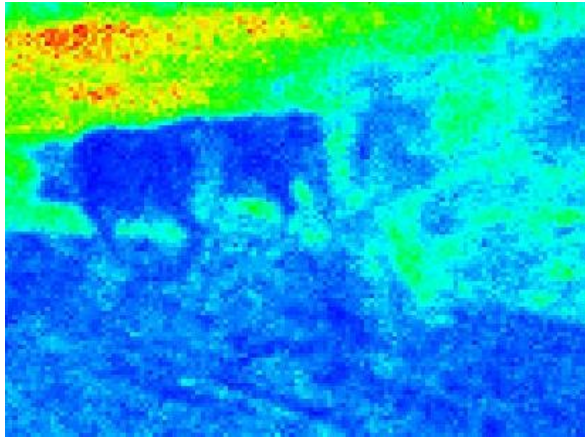
Copper K alfa



Barium L alfa



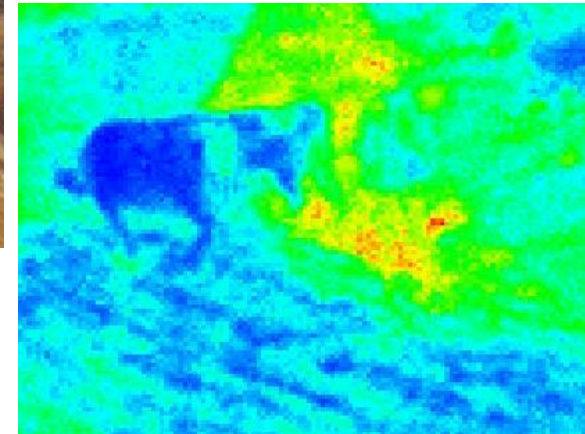
Total counts



Cromium K alfa



Visible



Lead L alfa







